Available online at www.sciencedirect.com
SCIENCE DIRECT®
Inorganica Chimica Acta 358 (2005) 2943–2953
Inorganica Chimica Acta
www.elsevier.com/locate/ica

Preparation of [*meso*-tetraphenylchlorophinato]nickel(II) by stepwise deformylation of [*meso*-tetraphenyl-2,3-diformyl-secochlorinato]nickel(II): conformational consequences of breaking the structural integrity of nickel porphyrins

Christian Brückner [a,*], Michael A. Hyland [a], Ethan D. Sternberg [b], Jill K. MacAlpine [b], Steven J. Rettig [b], Brian O. Patrick [b], David Dolphin [b,*]

[a] *Department of Chemistry, University of Connecticut, Unit 3060, 55 North Eagleville Road, Storrs, CT 06269-3060, USA*
[b] *Department of Chemistry, University of British Columbia, 2036 Main Mall, Vancouver, BC, Canada V6T 1Z1*

Received 11 August 2004; accepted 6 September 2004

This contribution is dedicated to the memory of Rex Shepherd

Abstract

The stepwise, Wilkinson's catalyst-induced decarbonylation of [*meso*-tetraphenyl-2,3-diformylsecochlorinato]Ni(II) (**4**) to produce the monoformylated pigment [*meso*-tetraphenyl-2-formylsecochlorinato] (**5**) and [*meso*-tetraphenylchlorophinato]Ni(II) (**6**) is described. Thus, we have shown how to degrade one pyrrolic unit of the starting material, [*meso*-tetraphenylporphyrinato]Ni(II) (**2**) in three steps to an aldimine linkage. The conformational changes of the porphyrinic macrocycle during the course of this degradation, as determined by comparison of the X-ray crystal structures of the compounds, are discussed. A comparative study delineates the UV–Vis spectroscopical consequences. In addition, the chemical reactivity of [*meso*-tetraphenylchlorophinato]Ni(II) (**6**) suggests the existence of an azepine-derived pyrrole-modified porphyrins (**11**, **12**).
© 2004 Elsevier B.V. All rights reserved.

Keywords: Nickel(II) porphyrin conformation; Ruffling; Porphyrins; Secochlorins; Chlorophins; Wilkinson's catalyst

1. Introduction

Nature fine-tunes the electronic properties and reactivity of porphyrinic co-factors by adjusting their degree of non-planarity [1–3]. Inter alia, the deformation of a porphyrinic chromophore from planarity causes a bathochromic shift in their UV–Vis absorption spectra although the exact cause for this shift is still a matter of discussion [4–6]. Investigations toward the fundamental understanding of non-planar porphyrins help to design long-wavelength absorbing photosensitizers and provide means to the understanding of porphyrinic co-factors in a range of enzymes and the light harvesting apparatus [1,2,7–9]. Non-planar porphyrins have also been utilized as chirality-memory molecules [10].

Synthetic non-planar porphyrins are traditionally generated by sterically crowding the porphyrin periphery [2,9]. The formal replacement of a pyrrolic building block in porphyrins by a larger, and possibly partially saturated, non-pyrrolic heterocycle offers another possibility to generate other non-planar porphyrinic chromophores.

* Corresponding authors. Tel.: +1 860 486 2743; fax: +1 860 486 2981 (C. Brückner), Tel.: +1 604 822 4571; fax: +1 604 822 9678 (D. Dolphin).
E-mail addresses: c.bruckner@uconn.edu (C. Brückner), ddolphin@qltinc.com (D. Dolphin).

0020-1693/$ - see front matter © 2004 Elsevier B.V. All rights reserved.
doi:10.1016/j.ica.2004.09.015

We and others, using different synthetic methodologies, have provided examples of such macrocycles although their conformation are not known in all cases [11–17]. We demonstrated the unique spectroscopic and electrochemical properties which distinguish pyrrole-modified porphyrins from porphyrins and chlorins [14–19].

It is well known that the introduction of Ni(II) into a porphyrin may cause some ruffling of the macrocycle, particularly when the ruffling also relieves steric crowding of peripheral substituents [7,20]. This observation finds an explanation in the relatively small ionic size of square planar Ni(II) (0.79 Å) [21] as compared to the size of the porphyrin cavity. The best measure for the size missmatch are the resulting relatively long Ni(II)–N bond distances in Ni(II) porphyrins. The long Ni(II)–N bonds in **1**, in turn, result in the ion 'pulling' the central nitrogens toward the center. The macrocycle responds to this force with a ruffling distortion of the ring. Although the ruffling distorts the conformation of the sp^2 ring atoms from planarity, thereby reducing their π-overlap, the loss in resonance energy and increase in strain energy is balanced by a stronger Ni–N bond [22]. Irrespective of the extent of the ruffling, however, this distortion mode does not alter the near-perfect square planar coordination environment around the metal center [2,7].

The Ni–N bond distances in the planar parent [porphyrinato]Ni(II) complex are 1.951 Å [23] while those in the slightly ruffled [*meso*-tetraphenylporphyrinato]Ni(II) (**1**) are 1.931 Å (RMS = 0.263 Å) [24]. This intrinsic ruffling of Ni(II) porphyrins is well understood and appropriate basis sets for their computational description were developed [25]. The average Ni(II)–N bond distance found in bis[(*meso*-phenyldipyrrinato)]Ni(II) (**2**) is 1.879 Å [26]. This complex can be viewed as porphyrin **1** lacking two *meso*-carbons and the rigidity these carbons impose onto the macrocycle. Hence, there a fewer structural restriction for the metal center to achieve ideal bond distances. Indeed, the bond distances measured in **2** are representative for the average bond lengths found for square planar diamagnetic Ni(II)–$N_{aromatic}$ bond distances (1.88 Å) [7]. [1]

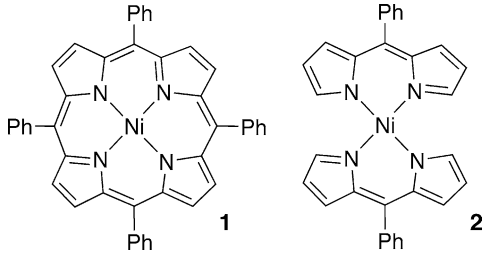

The extent of the ruffling the central metal can induce is dependent on the flexibility of the macrocycle and whether peripheral substituents also enforce a non-planar (ruffled) conformation. An empirical study of the conformation of thirteen Ni(II) complexes of hydroporphyrinoids was undertaken [7]. The study demonstrated, broadly speaking, that an increasing degree of saturation of the macrocycle correlated with an increasing degree of deformation from planarity. In other words, the larger the conjugated π-system, the stiffer the macrocycle, resulting in a more planar conformation and larger Ni(II)–N bond distances. The changes of the Ni(II)–N bond distances were also shown to modulate the electrophilicity of the central Ni(II) ion toward axial ligation. This observation served as the basis for the establishment of structure–function relationships of coenzyme F430 (a Ni(II) hydrocorphinato complex), and by implication, of coenzyme B_{12}. These implications were later refined and advanced by sophisticated experiments and calculations [8,27–29]. Interestingly, only one family of Ni(II) chlorins are found in nature, namely the tunichlorins [30]. However, the biological function of the tunichlorins in their host organism (tunicates, sea squirts) remains a mystery.

This rigidity of porphyrins is a consequence of their structurally very stable symmetric framework structure and extended π-system. What then are the conformational consequences of breaking the structural integrity of Ni(II) porphyrins by, β,β′-bond cleavage rather than mere β,β′-bond saturation? What are the practical limits of a Ni(II)-induced ruffling in porphyrinic chromophores of compromised structural rigidity? Can the ideal Ni–N bond distances for Ni(II) be achieved by an extremely ruffled porphyrinoid? This contribution will provide answers to these questions.

Following our preliminary communication [31], we present here a full report on the investigation of the step-wise degradation of [*meso*-tetraphenyl-2,3-*vic*-diolchlorinato]Ni(II) (**3**) via secochlorin **4**, monoformylchlorophin **5** to [*meso*-tetraphenylchlorophinato]Ni(II) (**6**) (Scheme 1). A comparison of the X-ray crystallographically determined conformations of **4**, **5**, and **6** with those of **1** and the [morpholinochlorinato]Ni(II) (**7**) [31] will allow conclusions on the conformational effects of Ni(II) on porphyrinic macrocycles of significant lesser structural integrity than porphyrins or chlorins. We also compare the combined effects of substituents and conformation on the electronic spectra of these chromophores. Lastly, we report on some notable observations regarding the chemical reactivity of **5** and **6**.

2. Experimental

2.1. Methods and materials

All solvents and reagents used were reagent grade or better and were used as received. The analytical TLC

[1] Average Ni–N distance in square planar Ni(II) complexes with aromatic nitrogen donor atoms is 1.88 Å. Cambridge Crystal Structure Data Base, CSD Version 5.24, November 2002.

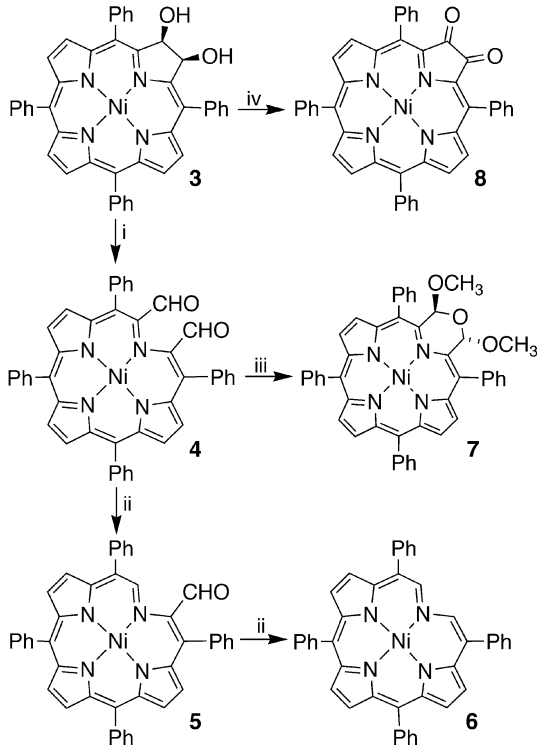

Scheme 1. *Reaction conditions*: (i) Pb^{IV} acetate, THF, 25 °C [14]; (ii) $(Ph_3P)_3RhCl$, PhCN, reflux; (iii) MeOH, CH_2Cl_2, $[H^+]$ [14]; (iv) DDQ, Δ [40].

plates were Silicycle ultra pure silica gel 60 (aluminum backed, 500 μm); preparative TLC plates (2–5 mm silica gel on glass) and the flash column silica gel (standard grade, 60 Å, 32–63 mm) used were provided by Sorbent Technologies, Atlanta, GA. Centrifugally accelerated chromatography using a Chromatotron™ (5 mm silica gel, gypsum binder, no fluorescence indicator) was also used for the separation of the products. ^1H and ^{13}C NMR spectra were referenced to residual solvent peaks. UV–Vis spectra were recorded on a Cary 50 spectrophotometer and IR spectra on a Perkin-Elmer Model 834 FT-IR. APCI+ mass spectra were recorded at the University of Connecticut (UConn) on a Micromass Quattro II using the conditions indicated. High-resolution FAB mass spectra were provided by the departmental Mass Spectrometry Facility at the University of British Columbia (UBC). Elemental analyses were provided by Numega Resonance Labs, Inc., San Diego, CA and the Departmental Elemental Analysis Laboratory at UBC.

Diol chlorinato Ni(II) complex **3** was prepared by OsO_4-mediated dihydroxylation of *meso*-tetraphenylporphyrin, followed by metal insertion [14,32]. Diformylsecochlorinato Ni(II) complex **4** was prepared by Pb^{IV}-induced diol cleavage of **3**, as described previously [14].

2.2. X-ray crystal structure determination of 5

The crystal structure analysis was performed at the X-Ray Crystallography Laboratories at UBC. Dark purple platelet crystals of $C_{43}H_{28}N_4ONi$, formula weight 675.40, crystallized by vapor phase diffusion of pet ether 30–60 into a solution of **5** in $CHCl_3$, having approximate dimensions of $0.25 \times 0.15 \times 0.08$ mm were mounted on a glass fiber. Data were collected on a Rigaku/ADSC CCD area detector with graphite monochromated Mo Kα radiation ($\lambda = 0.71069$ Å) at -100 ± 1 °C, using 0.50° oscillations with 51.0 s exposures. A sweep of data were done using ϕ oscillations from 0.0° to 190° at $\chi = -90°$, and a second sweep was performed using ω oscillations between −18.0° and 23.0°. Crystal-to-detector distance was 39.75 mm, the detector swing angle was −5.58°. Cell constants based on 9807 reflections with $2\Theta = 4.4$–$55.8°$ corresponded to a primitive triclinic cell with dimensions: $a = 11.6237(4)$ Å, $b = 11.7772(4)$ Å, $c = 13.2412(9)$ Å, $\alpha = 104.451(2)°$, $\beta = 98.010(2)°$, $\gamma = 90.489(2)°$, $V = 1736.4(1)$ Å^3, for $Z = 2$. The calculated density is 1.29 g/cm^3. Based on a statistical analysis of the intensity distribution, and the successful solution and refinement of the structure, the space group was determined to be $P\bar{1}$ (#2). Data were collected and processed using the d*TREK program [33]. A total of 15295 reflections were recorded, of which 6792 were unique ($R_{int} = 0.034$), equivalent reflections were merged. The linear absorption coefficient μ was 5.98 cm^{-1}, and data were corrected for Lorentz and polarization effects. Neutral atom scattering factors were taken from Cromer and Waber [34]. Anomalous dispersion effects were included in Fcalc with the values for $\Delta f'$ and $\Delta f''$ taken from Creagh and McAuley [35]. The values for the mass attenuation effects were those of Creagh and Hubbell [36]. All calculations were performed using the teXsan crystallographic package [37]. The structure was solved by direct methods and expanded using Fourier techniques. All non-hydrogen atoms were refined anisotropically. Hydrogen atoms were included but not refined. There is evidence for solvent included in the lattice, however, the degree of disorder made it impossible to properly identify or model this solvent. As a result, the program PLATON was used to correct the original data for the electron density from the disordered solvent [38]. The final cycle of full-matrix least-squares refinements was based on 6792 observed reflections with $I > 0.00\sigma(I)$ and 442 variables parameters and converged with unweighted and weighted agreement factors of $R_1 = 0.044$ and $\omega R_2 = 0.108$, respectively. Goodness-of-fit indicator $S = 1.05$. Maximum/minimum residual electron density in final difference Fourier map = 0.54 and −0.30 e$^-$/Å^3. Fig. 1 shows an ORTEP representation of the structure and the numbering scheme used. Table 1 lists selected bond distance, bond angles and dihedral angles found in **5**.

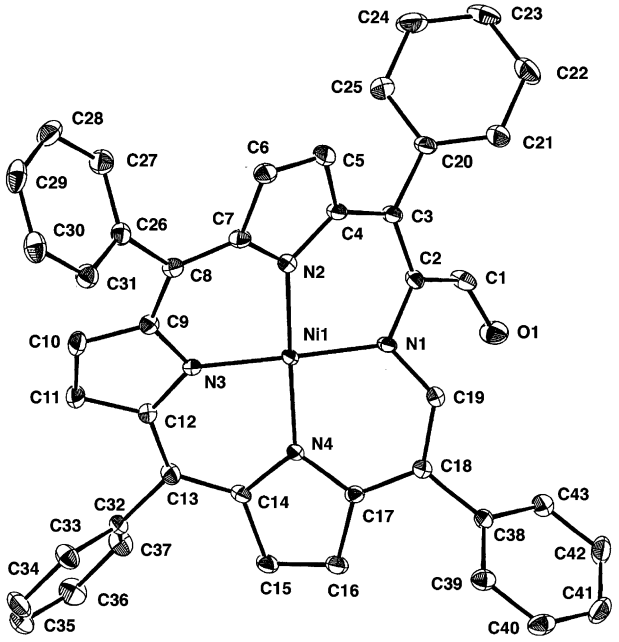

Fig. 1. ORTEP representation of **5**.

2.3. Deformylation of [2,4-diformyl-1,5,10,15-tetraphenylchlorophinato]nickel(II) (4)

A solution of brown [2,4-diformyl-1,5,10,15-tetraphenylchlorophinato]nickel(II) (**4**) (375 mg, 0.5 mmol) in anhydrous benzonitrile (60 mL) was treated with $(Ph_3P)_3RhCl$ (Wilkinson's catalyst, 900 mg, 2 mmol). Note: The reaction proceeded cleanly only with very dry benzonitrile (distilled over CaH_2 and stored over activated 4 Å molecular sieves). The reaction mixture was heated to reflux until all the starting material was consumed (up to 90 min reaction time). TLC control: R_f (**4**) = 0.60 (silica–toluene). In some runs it was necessary to add more of the catalyst to drive the reaction to completion. The solution was evaporated to dryness in vacuo and the green residue was purified by preparative thin layer chromatography (silica–toluene/hexane 3:1), allowing the isolation of the monodecarbonylated product **5** in 12% (40 mg) and chlorophin **6** in 59% (190 mg) yield. Workup of the reaction mixture before all the starting material is consumed, results in the recovery of **4**, and the isolation of a larger ratio of **5** to **6**.

2.4. [2-formyl-1,5,10,15-tetraphenylchlorophinato]nickel(II) (5)

R_f = 0.77 (silica–toluene); m.p. > 200 °C (d); ^1H NMR (400 MHz, $CDCl_3$) δ 7.42 (dd, J = 7.5, 1.0 Hz, 2H), 7.55–7.65 (m, 16H), 7.78 (d, J = 4.8 Hz, 1H), 7.95 (d, J = 7.1 Hz, 2H), 8.05, (d, J = 4.8 Hz, 1H), 8.07 (d, J = 4.8 Hz, 1H), 8.15 (d, J = 4.7 Hz, 1H), 8.22 (d, J = 4.9 Hz, 1H), 8.28 (d, J = 5.0 Hz, 1H), 9.80 (s, 1H), 9.85 (s, 1H); IR (film on KBr) 1657 (s, $\nu_{C=O}$) cm^{-1}; UV–Vis (CH_2Cl_2) λ_{max} (log ε): 448 (4.66), 630 (sh), 678 (3.90) nm; LR MS (EI^+) *m/e* (%) 674 (M^+, 100), 646 (M^+–CO, 85), 597 (M^+–C_6H_5, 55), 568 (M^+–C_6H_6–

Table 1
Selected bond distances (Å) and bond angles (°), and dihedral angles (°) found in **5**

Bond distances (Å)	
Ni1–N1	1.8960(17)
Ni1–N2	1.9034(17)
Ni1–N3	1.8964(17)
Ni1–N4	1.8930(16)
O1–C1	1.212(3)
N1–C2	1.398(3)
N1–C19	1.344(2)
N2–C4	1.360(3)
N2–C7	1.379(3)
N3–C9	1.383(3)
N3–C12	1.375(3)
N4–C14	1.384(3)
N4–C17	1.372(2)
C1–C2	1.480(3)
C2–C3	1.382(3)
C3–C4	1.410(3)
C4–C5	1.428(3)
C5–C6	1.361(3)
C6–C7	1.435(3)
C7–C8	1.397(3)
C8–C9	1.405(3)
C9–C10	1.424(3)
C10–C11	1.361(3)
C11–C12	1.432(3)
C12–C13	1.406(3)
C13–C14	1.385(3)
C14–C15	1.440(3)
C15–C16	1.356(3)
C16–C17	1.443(3)
C17–C18	1.395(3)
C18–C19	1.387(3)
Bond angles (°)	
N1–Ni1–N2	89.68(7)
N1–Ni1–N3	176.35(8)
N1–Ni1–N4	90.02(7)
N2–Ni1–N3	90.54(7)
N2–Ni1–N4	175.07(7)
N3–Ni1–N4	90.07(7)
C2–N1–C19	113.28(16)
N1–C2–C1	117.78(17)
O1–C1–H1	116.57
Torsion angles (°)	
C19–N1–C2–C1	43.9(3)
C19–N1–C2–C3	−143.2(2)
C2–N1–C19-C18	−157.5 (2)
O1–C1–C2–N1	−15.9(3)
O1–C1–C2–C3	170.9(2)
C4–C3–C20-C21	130.7(2)
C2–C3–C20-C25	130.4(2)
C7–C8–C26-C27	55.2(3)
C9–C8–C26–C27	−118.6(2)
C12–C13–C32–C33	−56.4(3)
C14–C13–C32–C37	−63.0(3)
C17–C18–C38–C43	126.0(2)
C19–C18–C38–C43	−44.3(3)

CO, 72), 492 (M^+–2 C_6H_5–CO, 35); HR MS (EI^+) *m/e* calculated for $C_{43}H_{28}N_4{}^{58}NiO$: 674.16168, found: 674.16024; LR MS (APCI+, 100% CH_3CN) *m/e* 674 (M^+). Elemental *Anal.* Calc. for $C_{43}H_{28}N_4NiO$ (from CH_2Cl_2/hexane): C, 76.47; H, 4.18; N, 8.30. Found: C, 75.32; H, 4.15; N, 8.20%.

2.5. [1,5,10,15-tetraphenylchlorophinato]nickel(II) (6)

R_f = 0.86 (silica–toluene); m.p. > 310 °C (sublimation); ^1H NMR (400 MHz, $CDCl_3$) δ 7.49 (tt, J = 7.2, 1.1 Hz, 1H), 7.55–7.65 (m, 5H), 7.78 (d, J = 7.7 Hz, 2H), 7.86 (dd, J = 7.6, 1.8 Hz, 2H), 8.15 (s, 1H), 8.20 (d, J = 4.8 Hz, 1H), 8.38 (d, J = 5.0 Hz, 1H), 9.80 (s, 1H); ^{13}C NMR (75 MHz, $CDCl_3$) δ 112.4, 123.8, 126.0, 127.0, 127.4, 128.2, 128.9, 129.2, 130.5, 131.8, 132.3, 133.2, 134.0, 134.7, 138.2, 138.9, 139.8, 140.3, 141.2, 141.6, 145.6; UV–Vis (CH_2Cl_2) λ_{max} (log ε): 422 (4.33), 576 (3.28), 612 (3.58) nm; IR (film on KBr): 3400 (s, CH_{Ar} stretch), 1570 (w, C=C), 1050 (m) cm^{-1}; LR MS (EI) *m/e* (%) 646 (M^+, 100), 568 (M^+–C_6H_6, 18); HR MS (EI^+) *m/e* calculated for $C_{42}H_{28}N_4{}^{58}Ni$: 646.16675, found: 646.16675; LR MS (APCI+, 100% CH_3CN) *m/e* 646 (M^+); Elemental *Anal.* Calc. for $C_{42}H_{28}N_4Ni \cdot H_2O$ (from CH_2Cl_2/wet MeOH): C, 75.81; H, 4.54; N, 8.42. Found: C, 75.89; H, 4.55; N, 8.30%.

3. Results and discussion

3.1. Stepwise degradation of [meso-tetraphenyl-2,3-diformyl-secochlorinato]Ni(II) (4) to [meso-tetraphenyl chlorophinato]Ni(II) (6)

[*meso*-Tetraphenylsecochlorinato]Ni(II) bisaldehyde **4**, accessible by Pb^{IV}-induced cleavage of β,β′-diol chlorin **3** [14], is, like many other aromatic aldehydes, susceptible to a step-wise decarbonylation reaction catalyzed by Wilkinson's catalyst, $(Ph_3P)_3RhCl$ (Scheme 1) [39]. Thus, a solution of yellow-brown **4** in benzonitrile, when reacted with a stoichiometric excess of $(Ph_3P)_3RhCl$ under reflux, produced successively the monodecarbonylated brown-green product **5** and the bis-decarbonylated green [*meso*-tetraphenylchlorophinato]Ni(II) (**6**). Upon consumption of the starting material, chromatographic separation of the reaction mixture allowed the isolation of crystalline **5** (12%) and **6** in up to 60% yield. Incomplete conversion of **4** produced a larger fraction of **5**, making up to 40% of the reaction mixture, and some of the starting material could be recovered. The reaction is very clean and only traces of other pigments are generated (vide infra).

The HR mass spectra (EI^+) of the pigments (**5**: *m/e* calculated for $C_{43}H_{28}N_4NiO$: 674.16168, found: 674.16024; **6**: *m/e* calculated for $C_{42}H_{28}N_4Ni$: 646.16675, found: 646.16675) as well as elemental analysis data corroborate the proposed compositions. Whereas the IR spectra of **4** and **5** indicate the presence of a carbonyl group (strong $\nu_{C=O}$ bands at 1684 and 1657 cm^{-1}, respectively), no such band is observable for **6**. A comparison of the ^1H NMR spectra of **4**, **5**, and **6** show the stepwise loss of the signals attributed to the carbonyl group (**4**: δ 9.50 ppm; **5**: δ 9.85 ppm) and its concomitant replacement by a singlet at δ 9.80 ppm with an integration corresponding to 1H and 2H for **5** and **6**, respectively. We assign this signal to the α-proton which appears as the result of the decarbonylation. The diatropic shift for the α-protons is comparable to those measured for *meso*-protons of other porphyrins such as 5,15-diphenylporphyrin [41]. The loss of the twofold symmetry of **4** when loosing one carbonyl group and the reestablishment of the twofold symmetry upon loss of the second carbonyl group is also clearly observed in the β-region (δ 8.0–8.5 ppm) of the spectra. The twofold symmetric secochlorin **4** (two doublets and one singlet in a 1:1:1 ratio) turns into monocarbonyl **5** with no rotational symmetry (displaying six doublets in a 1:1:1:1:1:1 ratio). Loss of the second carbonyl group generates the twofold symmetric chlorophin **6** (again, displaying two doublets and one singlet in a 1:1:1 ratio). Overall, the step-wise degradation of the ultimate starting material TPPNi (**1**) in three steps (dihydroxylation, diol cleavage, decarbonylation) is straight forward, simple and high yielding.

The synthesis of the tetraphenylchlorophin (**6**) [11] as well as the parent chlorophin (i.e. the non-*meso*-phenyl substituted macrocycle) [42] have been unsuccessfully attempted before. Two other related pigments were reported by Flitsch and co-workers [43]. These are the bacteriochlorin and isobacteriochlorin analogs of parent chlorophin **6**. In contrast to our facile preparation of **6**, however, their total syntheses were extremely difficult and very low yielding (≪0.1% over several steps), and no structural characterization was accomplished.

Unlike the developed chemistry of the secoporphyrazines [44], examples of porphyrin-derived secochlorins are rare [13,45,46]. However, the β,β′-bond of the parent porphyrin or chlorin that was cleaved was in all these cases alkylated, methoxy- or amine-substituted. Bond cleavage thus generated ketone-, ester- or amide-functionalized secochlorins or secoporphyrazines, respectively, which did not lend themselves to the degradation pathways demonstrated here.

3.2. Conformational analysis of the products

Single-crystal X-ray diffraction studies on secochlorin bisaldehyde **4**, monoaldehyde **5**, and chlorophin **6** were performed [31], and the structure of **5** is reported for

the first time here. [2] The results of this structural determination unequivocally prove the assigned structures (Fig. 1, Scheme 1). Thus, one pyrrolic unit of the parent porphyrin was step-wise degraded to an aldimine linkage, without any other change in the connectivity of the macrocycle.

The plane of the metallosecochlorins, while retaining a square planar coordination sphere around the central metal, are severely twisted along an N–Ni–N axis resulting in a ruffled conformation of the porphyrin core, with a decreasing degree of ruffling with the removal of the formyl groups (RMS of the $C_{18}N_4Ni$ mean plane: 0.465 Å in **4**, 0.391 Å in **5**, and 0.368 Å in **6**, respectively) [47,48]. Parallel to the decreasing ruffling, the mean Ni–N bond distances are lengthened, from 1.892 Å measured in **4** to 1.910 Å in **6**. The longest individual bond length in each compound is, analogous to precedents in the solid state structures of [chlorinato]Ni(II) complexes, found between the metal and the nitrogen of the imine unit (Table 1) [49]. The short bond length observed in **4** is near the ideal Ni–N bond length observed in dipyrrinato complex **2** [26] or the average Ni–N distance of sterically unencumbered Ni(II) complexes with imine type ligands (approximately 1.85 Å) [50]. They are shorter than observed for even extremely distorted [porphyrinato]Ni(II) complexes [9], [hydroporphyrinato]Ni(II) complexes [7], and are comparable to those observed in the Ni(II) complexes of hydrocorrins, macrocycles lacking one *meso*-ring carbon as compared to our systems [51]. Since the median Ni–N distances have been used, among other measurements, to quantify the distortion of porphyrins [20], the chromophores of **4** (and **7**) qualify as the most distorted porphyrinic structures to date.

Observation of the extremely ruffled conformation and the concomitant short Ni–N bond distances highlight the compromised rigidity of porphyrinic systems with a broken β,β′-bond. The pronounced influence of the formyl substituents on the degree of the ruffling is, perhaps, surprising. Evidently, they assist in the ruffling distortion although they cannot be considered to sterically encumbering the porphyrin periphery. The conformation of **4** allows the formyl moieties to be arranged parallel to each other, allowing for π–π-stacking interactions (average distance of the C═O bonds: 2.85 Å) and for maximum conjugation with the porphyrinc π-system. However, these interactions should not be forceful enough to distort the pigment into the observed extremes, unless the chromophore is extraordinarily flexible. Monoformyl complex **5** shows an intermediate conformation between that of **4** and **6**.

Moreover, while the $C_{18}N_4Ni$ core of **4** and **6** are pseudo-twofold symmetric, the core of **5** is distinctly non-symmetric. The half opposite the one carrying the formyl group shows a larger degree of ruffling, and is super-imposable over the structure of the bisaldehyde **4**, while the other half carrying the formyl group is super-imposable over the structure of the chlorophin **6**.

The ruffled distortion allows the *meso*-phenyl groups to adopt a slightly more co-planar conformation with respect to the porphyrinic chromophore. While the dihedral angle along the phenyl *o*-C bonds, the *ipso*-C, the *meso*-C to nearest α-carbon in regular porphyrins are in the range of 80°, i.e. the phenyl groups are idealized orthogonal to the plane of the porphyrin, they are between 45° and 55° in the secochlorins **4** and **5** and the chlorophin **6**. [3] The near-orthogonal arrangement of the *meso*-phenyl groups in porphyrins finds its origin in the steric interaction between the *o*-phenyl hydrogens and the flanking β-hydrogens. Especially in chlorophin **6**, this steric interaction is removed on the side of the phenyl groups next to the imine linkage. Further, the ruffling relieves some of the remaining *o*-phenyl to β-hydrogen interactions.

We have previously shown that secochlorin **4** reacts under acidic conditions with simple alcohols to form [morpholinochlorinato]Ni(II) (**7**) (Scheme 1) [14]. The ruffled conformation of **7** is near-identical to that of **6** (RMS of the $C_{18}N_4Ni$ mean plane: 0.468 Å; Fig. 2). Later work has shown that the free base of **7** is only minimally ruffled (RMS of the $C_{18}N_4$ mean plane: 0.012 Å), indicating that the conformation of **7** is exclusively due to the templating ion and not, as initially assumed, also due to the morpholine ring fused into the macrocycle [19]. In fact, the conformation of the $C_{18}N_4Ni$ core in **7** is already preformed in **4**, and they are nearly perfectly superimposable.

3.3. Comparative study of the UV–Vis spectra of chromophores 3–8

A comparison of the UV–Vis spectra of the chromophores **3**–**8** is shown in Fig. 3. The spectrum of the [diolchlorinato]Ni(II) complex **3** is included as a benchmark [chlorinato]Ni(II) spectrum against which the conformational and electronic effects in the other chromophores can be evaluated. Its conformation is not known. However, projected from the conformations of **1**, **8** and other Ni(II) chlorins [8,52,53], **3** can reasonably assumed to be only moderately ruffled.

[2] The results of the structural analyses of **4** (GUBWAB), and **6** (GUBWEF), reported in our communication [33], have been deposited at the Cambridge Crystallographic Data Center under the codes indicated.

[3] The traditional measurement of the dihedral angle between the mean plane of the porphyrin chromophore and the phenyl group is less meaningful in these highly distorted systems.

The spectrum of dione **8**, prepared by oxidation of the diol **3** (Scheme 1) [40], is included since it possesses a [chlorinato]Ni(II)-type chromophore to which two carbonyl groups in β-positions are in conjugation with the macrocycle. The strong electronic influence of conjugated carbonyl groups on the UV–Vis spectrum of porphyrinic chromophores is well known [54–56], and as a comparison of the spectra of **3** and **8** clearly demonstrates. Further, the conformation of **8** was determined to be similar to that of the porphyrin **1** (for **8**, RMS = 0.293 Å) [40]. Thus, the differences of the spectra of **3** and **8** are largely due to the electronic effects of the two carbonyl groups. [Secochlorinato]Ni(II) bisaldehyde **4** also carries two carbonyl groups at equivalent β-positions to those in **8**, albeit they can rotate freely and, most importantly, the conformation of the macrocycle is dramatically distorted from planarity. [4] The cumulative effects of the non-planar conformation of the macrocycle and the two conjugated carbonyl groups result in a UV–Vis spectrum of **4** that shows similarities and differences with that of **8**. It also displays a 'double' Soret band but the intensity ratio of the two bands is inverted. Although less pronounced, **4** also features a red-shifted and broadened side band. Removal of one carbonyl group changes the conformation only slightly (RMS of 0.492 Å) but the UV–Vis spectrum of **5** is significantly different from that of **4**. The double-Soret band collapses into one (although a shoulder at ~410 nm is still evidence for the presence of two distinct transitions) and the side band gains definition and is slightly hypsochromically shifted.

The large difference between the spectra of **4** and **5** highlights again the strong electronic effect of the carbonyl substituents. Correspondingly, removal of the carbonyl group from **5** produces chlorophin **6** with a bathochromically shifted Ni(II) chlorin-type spectrum (Soret band is shifted by 6 nm as compared to the Soret band of **3**). This shift is likely due to the non-planarity of **5**. The comparison, however, neglects the electronic effects of the benzylic oxygens of **3** [57]. [Morpholinochlorinato]Ni(II) **7** also carries benzylic oxygens (albeit three as compared to two on **3**). A comparison of the spectrum of **7** with that of **3** and **6** is illustrative of the conformational effects. The chromophore of **7** is very non-planar (RMS of 0.468 Å). As a result, it displays a bathochromically shifted spectrum as compared to chlorin **3**.

The acid-induced demetallation of [secochlorinato]Ni(II) and [chlorophinato]Ni(II) complexes fails to provide the free base analogues. Instead, extensive decomposition is observed. Hence, no comparisons can be made with the free base analogs of **4**–**6**. Molecular modeling studies suggest, however, that the free base of **4** is perfectly planar [58].

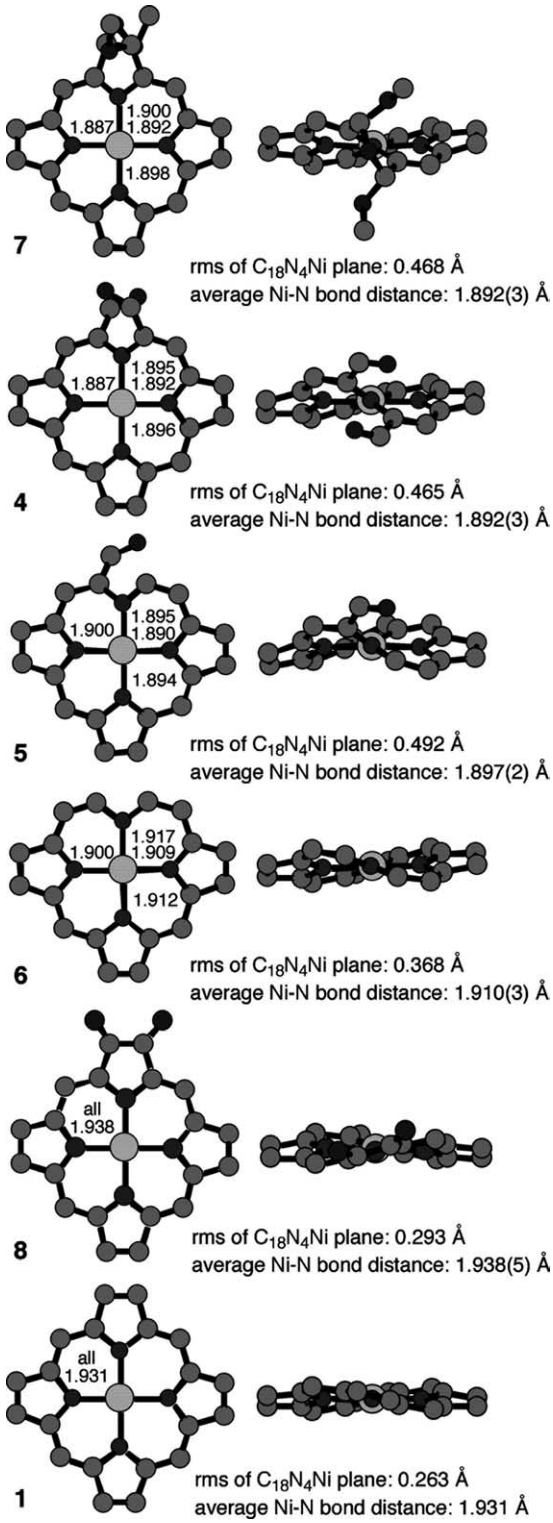

Fig. 2. Top view of and edge-on view (along the pseudo-twofold N–Ni–N axis) of the chromophores of **1**, **4**–**6**, and **7**. The Ni–N bond distances for **6** were determined by averaging the equivalent bond lengths of the two molecules present in the asymmetric unit.

[4] Shelnutt and co-workers [6] have shown that certain distortion modes contribute to a much larger extent to the modulation of the UV–Vis spectra of porphyrin than others. Therefore, the overall distortion of the macrocycle expressed in the root mean square (RMS) displacement from planarity is not necessarily the best measure for the conformational influence of the chromophore on the UV–Vis spectra.

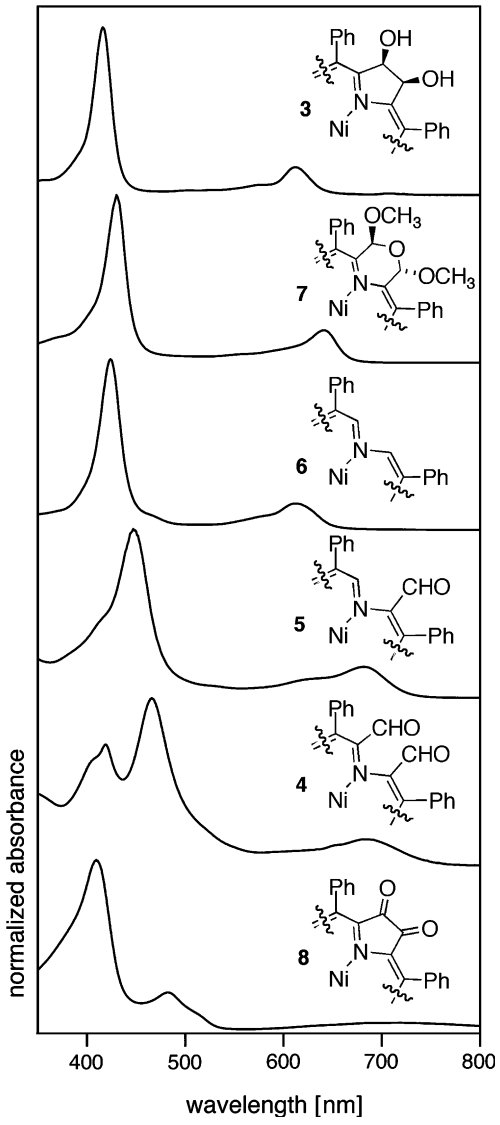

Fig. 3. Stacked plot of the normalized UV–Vis spectra of **3**–**8** ($CHCl_3$).

3.4. Chemical reactivity of 5 and 6

We have reported on the reactivity of [secochlorinato]Ni(II) **4** with respect to its conversion to **7** and related macrocycles [14–18]. Also, while attempting the acid-induced demetalation of **4**, we discovered the acid-catalyzed intramolecular electrophilic aromatic substitution of the *o*-phenyl hydrogens by adjacent formyl groups, resulting in the formation of indaphyrins [16,17], but the chemistry of secochlorin **5** and the chlorophin **6** remained hitherto unexplored.

Secochlorin monoaldehyde **5** is conceptually accessible via Vilsmeier–Haak formylation of **6**. For this reaction to lead to the expected product, however, the reactivity of the α-position toward electrophilic aromatic substitution needs to be more pronounced than those of the β-positions (formylation of the phenyl groups is not observed under these conditions [59]). Formylation of **6** under standard Vilsmeier–Haak conditions lead to the formation of monoformylated products, as seen by the occurrence of a strong peak at *m/e* = 674 in the APCI+ mass spectrum of the crude reaction mixture. Preparative plate chromatography of the mixture allowed the isolation of **5** as the main product (~30%). A second, slightly more polar, dark green fraction proved to be a mixture of compounds of identical mass (APCI+, *m/e* = 674). Due to their near-identical R_f values, the isolation of pure products failed. The ^1H NMR of the product mixture showed five singlets in the range of 9.5–9.8 ppm, indicative of formyl- and α-hydrogens. The spectrum also allowed the identification of at least eight signals (two singlets, six doublets with $J \approx 5$ Hz) in the β-hydrogen region of the spectrum (8.0–9.0 ppm), and showed a complex feature between 7.5 and 7.9 ppm, typical of the phenyl hydrogens. The relative integrated intensity of the peaks in the phenyl range vs. those in the low-filed region of the spectrum was 2.5:1. These data indicate that formylation has taken place over all (or at least several) available β-positions, leading to a mixture of (up to 4) regioisomers of **6** (**9**) (Scheme 2).

Next to the dark green formylation products of **6**, we noticed the appearance of a trace amount (estimated to be <3%) of a turquoise (λ_{max} = 411 and 608 nm, 1:0.23 intensity ratio), low polarity compound. Traces of this product were also found as one of the few side-products during the deformylation of **4**. A number of observations led us to speculate that this pigment is alcohol **11**. Its HR-FAB+ mass spectrum showed a peak at *m/e* = 674.1623, corresponding to $C_{43}H_{28}N_4NiO$ (expected *m/e*: 674.1617). EI+ and APCI+ spectra of **11** show as the most prominent peak the dehydroxylated species **13** (*m/e* = 657). This fragment represents a particularly well conjugated and stable carbocationic species. The ^1H NMR of **11** ($CDCl_3$, 300 MHz) is simple, reflecting the twofold symmetry of the molecule. The β-region of the spectrum (two overlapping d at 8.45 and 8.46 pp, J = 4.8 Hz, one s at 8.23 ppm, 1:1:1 integrated intensity ratio, 6H total) is clearly separated from the phenyl

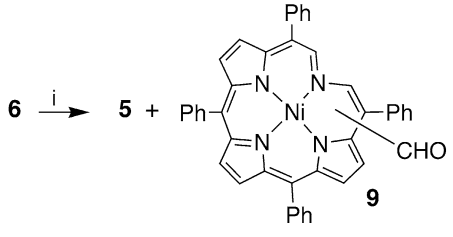

Scheme 2. Vilsmeier–Haak formylation of chlorophin **6**. *Reaction conditions*: (i) DMF/$POCl_3$, 0 °C, 20 min, then warming to 60 °C for 40 min, followed by aq $NaHCO_3$ quench; preparative TLC chromatography (silica–1:1 CH_2Cl_2:pet ether 30-60).

region (two d, $J = 8$ Hz at 7.94 and 8.00 ppm, 2H each, and multiplets at 7.36–7.43, 7.61–7.65, and 7.7–7.8 ppm, total of 20H). The two (complex) doublets, assigned to the *o*- and *o*′-hydrogens of the phenyl groups next to the four-membered ring, reflect the face differentiation of the single hydroxy functionality on the azepin ring. An equivalent face differentiation was shown to operate in the NMR spectrum of *vic*-diol chlorins [14]. Two further signals are of diagnostic value: One d (6.58 ppm, $J = 9$ Hz, 1H) and one br d at 2.88 ppm ($J = 9$ Hz, 1H), assigned to the protons of azepine CH(OH) group. These signal simplify upon treatment of the NMR sample with D_2O. The proton giving rise to the high field signal is exchangeable with D_2O and vanishes, and the low-field signal becomes a singlet. While all indications point toward the confirmation of our structural assignment of **11**, we were not able to prepare enough sample to further corroborate its structure. It should be noted, however, that Crossley and King [11] were the first to suggest, in 1984, the occurrence of a pyrrole-modified porphyrin containing a contracted, four-membered ring.

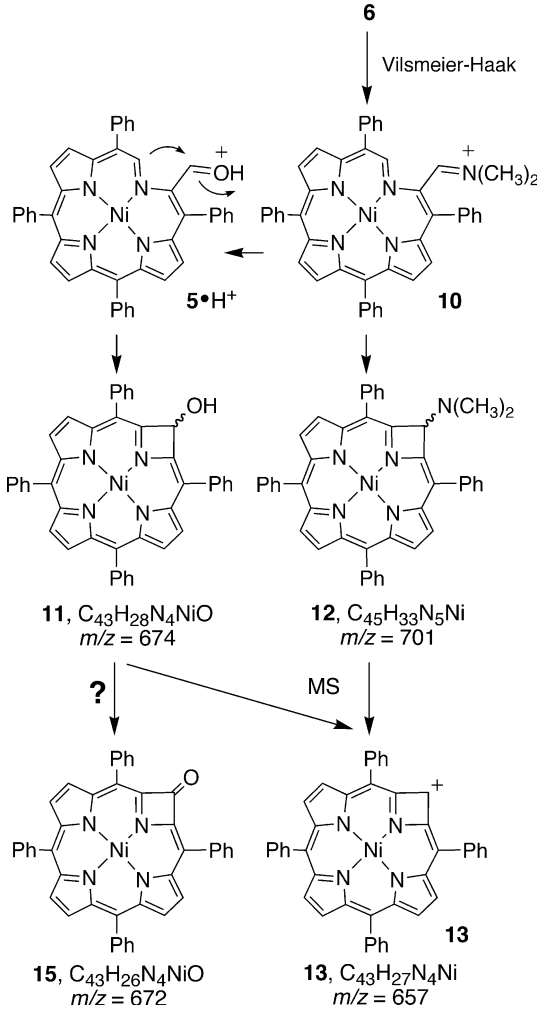

Scheme 3.

During the oxidative degradation of free base dioxoporphyrins they proposed the existence of ketone **15**. Perhaps somewhat surprisingly, we did not observe the spontaneous (air) oxidation of **11** to **15** during our studies of **11**.

Cation **13** is also observed in the APCI+ mass spectrum of an unquenched crude reaction mixture resulting from a Vilsmeier–Haak reaction of chlorophin **6**. Fractionation of the crude mixture showed that one pigment with a mass corresponding to **12**, was the origin of fragment **13**. Both azepin-derivatives **11** and **13** are perceivably derived from a similar mechanism. Either the primary Vilsmeier product, the imine **10**, or the (protonated) monoformyl secochlorin $\mathbf{5} \cdot H^+$ serve as intramolecular electrophiles in an electrophilic aromatic substitution reaction at the neighboring α-position (Scheme 3). This mechanism suggests that conditions could be found to convert **5** directly to **11**, a hypothesis we were not able to confirm.

4. Conclusions

We have shown how to degrade one pyrrolic unit of the initial starting material *meso*-tetraphenylporphyrin **2** in three steps (dihydroxylation, diol cleavage, decarbonylation) to an aldimine linkage. While other porphyrin degradation pathways have been reported before, mainly involving cleavages at the *meso*-position, this degradation of the β-positions is novel to the chemistry of porphyrins. A degradation of the β,β′-moiety of a porphyrazine diol chlorin was reported [44]. However, the mechanism of the degradation and the resulting product, a seco-chlorin-type chromophore incorporating a urea-like functionality, vary from those reported here. The X-ray crystal structure determination of **4**, **5**, and **6** revealed their severe ruffled conformations. The driving force for the deviation of the porphyrinic chromophores from planarity lie in the achievement of ideal Ni–N bond distances, assisted by the formyl substituents. Substituents may accentuate this twist, as seen in the more pronounced twist in **4** and **7** as compared to that seen in **6**.

While the conformational effects of the coordination of Ni(II) to porphyrinic macrocycles is well known, they were hitherto not demonstrated in systems lacking a β,β′-bond. It can be concluded that no significantly larger degree of Ni(II)-induced ruffling of a porphyrinic chromophore than that observed in **4** and **7** can be achieved because the ideal Ni(II)–N bond distances are attained in these systems. Furthermore, the electronic effects of the formyl substituents on the UV–Vis spectra of the chromophore are strong and override the more subtle conformational effects.

The chemical reactivity of the secochlorins remains to be further explored but evidence was gathered for the

existence of the intriguing pyrrole-modified porphyrin **14** in which one pyrrolic unit of a porphyrin was formally replaced by anazetin moiety. Work regarding the reactivity of secochlorins continues to be explored in our laboratories.

5. Supplementary material

Complete crystallographic data (excluding structure factors) for the structure of monoformyl [secochlorinato]Ni(II) **5** have been deposited at the Cambridge Crystallographic Data Centre, CCDC #244651. Copies of the data can be obtained free of charge on application to: The Director, CCDC, 12 Union Road, Cambridge CB2 1EZ, UK (fax: +44 1223336 033, email: deposit@ccdc.cam.ac.uk or www: http://www.ccdc.cam.ac.uk).

Acknowledgements

This work was supported by the University of Connecticut Research Foundation (UCRF) and the Natural Science and Engineering Research Council (NSERC), Canada.

References

[1] M. Ravikanth, T.K. Chandrashekar, Struct. Bond. (Berlin) 82 (1995) 107.
[2] J.A. Shelnutt, X.-Z. Song, J.-G. Ma, W. Jentzen, C.J. Medforth, Chem. Soc. Rev. 27 (1998) 31.
[3] E. Sigfridsson, U. Ryde, J. Biol. Inorg. Chem. 8 (2002) 273.
[4] A.K. Wertsching, A.S. Koch, S.G. DiMagno, J. Am. Chem. Soc. 123 (2001) 3932.
[5] H. Ryeng, A. Ghosh, J. Am. Chem. Soc. 124 (2002) 8099.
[6] R.E. Haddad, S. Gazeau, J. Pécaut, J.-C. Marchon, C.J. Medforth, J.A. Shelnutt, J. Am. Chem. Soc. 125 (2003) 1253.
[7] C. Kratky, R. Waditschatka, C. Angst, J.E. Johansen, J.C. Plaquevent, J. Schreiber, A. Eschenmoser, Helv. Chim. Acta 68 (1985) 1313.
[8] T. Wondimagegn, A. Ghosh, J. Phys. Chem. B 104 (2000) 10858.
[9] M.O. Senge, in: K.M. Kadish, K.M. Smith, R. Guilard (Eds.), The Porphyrin Handbook, Academic Press, San Diego, 2000, pp. 239–248.
[10] (a) See e.g.: Y. Furusho, T. Kimura, Y. Mizuno, T. Aida, J. Am. Chem. Soc. 119 (1997) 5267;
(b) Y. Mizuno, T. Aida, K. Yamaguchi, J. Am. Chem. Soc. 122 (2000) 5278;
(c) Y. Kubo, T. Ohno, J. Yamanaka, S. Tokita, T. Iida, Y. Ishimaru, J. Am. Chem. Soc. 123 (2001) 12700;
(d) For the chiral resolution of a non-planar porphyrins, see: H.W. Daniell, C. Brückner, Angew. Chem. Int. Ed. 43 (2004) 1688.
[11] M.J. Crossley, L.G. King, J. Chem. Soc., Chem. Commun. (1984) 920.
[12] T.D. Lash, in: R. Guilard (Ed.), The Porphyrin Handbook, Academic Press, San Diego, 2000, pp. 125–200.
[13] (a) K.R. Adams, R. Bonnett, P.J. Burke, A. Salgado, M.A. Vallés, J. Chem. Soc. Perkin Trans. 1 (1997) 1769;
(b) K.R. Adams, R. Bonnett, P.J. Burke, A. Salgado, M.A. Vallés, J. Chem. Soc., Chem. Commun. (1993) 1860.
[14] C. Brückner, S.J. Rettig, D. Dolphin, J. Org. Chem. 63 (1998) 2094.
[15] J.R. McCarthy, P.J. Melfi, S.H. Capetta, C. Brückner, Tetrahedron 59 (2003) 9137.
[16] J.R. McCarthy, M.A. Hyland, C. Brückner, Chem. Commun. (2003) 1738.
[17] J.R. McCarthy, M.A. Hyland, C. Brückner, Org. Biomol. Chem. 2 (2004) 1484.
[18] C.J. Campbell, J.F. Rusling, C. Brückner, J. Am. Chem. Soc. 122 (2000) 6679.
[19] J.R. McCarthy, H.A. Jenkins, C. Brückner, Org. Lett. 5 (2003) 19.
[20] K.M. Barkigia, M.W. Renner, L.R. Furenlid, C.J. Medforth, K.M. Smith, J. Fajer, J. Am. Chem. Soc. 115 (1993) 3627.
[21] R.D. Shannon, Acta Crystallogr., Sect. A 32 (1976) 751.
[22] The Ni–N bond strength in **1** is, however, by no means weak. The demetallation of **1** requires conc. H_2SO_4 at 25 °C for 2 h, see e.g., J.W. Buchler, in: K.M. Smith (Ed.), Porphyrins and Metalloporphyrins, Elsevier, Amsterdam, 1975, pp. 197–201.
[23] W. Jentzen, I. Turowska-Tyrk, W.R. Scheidt, J.A. Shelnutt, Inorg. Chem. 35 (1996) 3559.
[24] E.B. Fleischer, C.K. Miller, L.E. Webb, J. Am. Chem. Soc. 86 (1964) 2342.
[25] P.M. Kozlowski, T.S. Rush, Iii, A.A. Jarzecki, M.Z. Zgierski, B. Chase, C. Piffat, B.-H. Ye, X.-Y. Li, P. Pulay, T. Spiro, J. Phys. Chem. A 103 (1999) 1357.
[26] Despite a dihedral angle of 42° between the dipyrrinato subunits, the Ni(II) center is low spin, diamagnetic. C. Brückner, V. Karunaratne, S.J. Rettig, D. Dolphin, Can. J. Chem. 74 (1996) 2182.
[27] W.A. Kaplan, K.S. Suslick, R.A. Scott, J. Am. Chem. Soc. 113 (1991) 9824.
[28] L.R. Furenlid, M.W. Renner, K.M. Smith, J. Fajer, J. Am. Chem. Soc. 112 (1990) 1634.
[29] T. Wondimagegn, A. Ghosh, J. Am. Chem. Soc. 123 (2001) 1543.
[30] (a) K.C. Bible, M. Buytendorp, P.D. Zierath, K.L. Rinehart, Proc. Natl. Acad. Sci. USA 85 (1988) 4582;
(b) G.R. Pettit, D. Kantoci, D.L. Doubek, B.E. Tucker, W.E. Pettit, R.M. Schroll, J. Nat. Prod. 56 (1993) 1981;
(c) H.L. Sings, K.C. Bible, K.L. Rinehart, Proc. Natl. Acad. Sci. USA 93 (1996) 10560.
[31] C. Brückner, E.D. Sternberg, J.K. MacAlpine, S.J. Rettig, D. Dolphin, J. Am. Chem. Soc. 121 (1999) 2609.
[32] C. Brückner, D. Dolphin, Tetrahedron Lett. 36 (1995) 3295.
[33] Area Detector Software, Version 4.13, Molecular Structure Corp., 1996–1998.
[34] D.T. Cromer, J.T. WaberInternational Tables for X-ray Crystallography, vol. IV, The Kynoch Press, Birmingham, 1974, Table 2.2 A.
[35] D.C. Creagh, W.J. McAuleyInternational Tables for X-ray Crystallography, vol. C, Kluwer Academic Publishers, Boston, 1992, Table 4.2.6.8.
[36] D.C. Creagh, J.H. HubbellInternational Tables for X-ray Crystallography, vol. C, Kluwer Academic Publishers, Boston, 1992, Table 4.2.4.3.
[37] teXsan: Crystal Structure Analysis Package, Molecular Structure Corp., 1985 and 1992.
[38] A.L. Spek, University of Utrecht, The Netherlands, 2000.
[39] R.L. Pruett, Adv. Organomet. Chem. 17 (1979) 1.
[40] H.W. Daniell, S.C. Williams, H.A. Jenkins, C. Brückner, Tetrahedron Lett. 44 (2003) 4045.
[41] C. Brückner, J.J. Posakony, C.K. Johnson, R.W. Boyle, B.R. James, D. Dolphin, J. Porphyrins Phthalocyanines 2 (1998) 455.
[42] M. Bohusch, W. Flitsch, H.-G. Kneip, Liebigs Ann. Chem. (1991) 67.

[43] (a) W. Flitsch, Pure Appl. Chem. 58 (1986) 153;
(b) W. Flitsch, D. Schulz, H.-G. Kneip, Liebings Ann. Chem. (1985) 1004;
(c) W. Flitsch, Adv. Heterocycl. Chem. 43 (1988) 73.
[44] (a) A.G. Montalban, S.M. Baum, A.G.M. Barrett, B.M. Hoffman, Dalton Trans. (2003) 2093;
(b) H. Nie, C.L. Stern, A.G.M. Barrett, B.M. Hoffman, Chem. Commun. (1999) 703.
[45] C.K. Chang, W. Wu, S.-S. Chern, S.-M. Peng, Angew. Chem., Int. Ed. Engl. 31 (1992) 70.
[46] J.L. Sessler, S.V. Shevchuk, W. Callaway, V. Lynch, Chem. Commun. (2001) 968.
[47] A full normal-coordinate structural decomposition (NSD) analysis of the structures gave unreasonably large values for the some of the distortion modes. This can be rationalized because the NSD requires an intact porphyrinic $C_{20}N_4$ macrocycle to provide data which are comparable to other non-planar porphyrins [48], thus, the results of a NSD are not reported.
[48] (a) W. Jentzen, X.-Z. Song, J.A. Shelnutt, J. Phys. Chem. B 101 (1997) 1684;
(b) W. Jentzen, J.-G. Ma, J.A. Shelnutt, Biophys. J. 74 (1998) 753.
[49] A.M. Stolzenberg, M.T. Steshic, J. Am. Chem. Soc. 110 (1988) 6391.
[50] K. Henrick, P.A. Tasker, L.F. Lindoy, Prog. Inorg. Chem. 33 (1985) 1.
[51] C. Angst, A. Kratky, A. Eschenmoser, Angew. Chem., Int. Ed. Engl. 20 (1981) 236.
[52] A. Ulman, J. Gallicci, D. Fisher, J.A. Ibers, J. Am. Chem. Soc. 102 (1980) 6852.
[53] K.M. Barkigia, M.A. Thompson, J. Fajer, R.K. Pandey, K.M. Smith, M.G.H. Vicente, New J. Chem. 16 (1992) 599.
[54] C.K. Chang, M.H. Hatada, A. Tulinsky, J. Chem. Soc. Perkin Trans. 2 (1983) 371.
[55] C.G. Chang, C. Sotiriou, J. Heterocyclic Chem. 22 (1985) 1739.
[56] C. Brückner, J.R. McCarthy, H.W. Daniell, Z.D. Pendon, R.P. Ilagan, T.M. Francis, L. Ren, R.R. Birge, H.A. Frank, Chem. Phys. 294 (2003) 285.
[57] The benzylic oxygens have a small but distinct effect as, for instance, the comparison of the UV–Vis spectra of diol chlorin **3** (λ_{max} = 644 nm) with that of the parent *meso*-tetraphenylchlorin (λ_{max} = 652) demonstrates. H.W. Whitlock Jr., R. Hanamer, M.Y. Oester, B.K. Bower, J. Am. Chem. Soc. 91 (1969) 7485.
[58] CAChe V4.9.2, MM4 force field, Fujitsu Ltd., 2003.
[59] J.W. Buchler, C. Dreher, G. Herget, Liebigs Ann. Chem. (1988) 43.